

Structure and reactions of the two-neutron halo nucleus ^{11}Li

K.O. Mendibayev^{1,2,*}, T. Issatayev^{1,2}

¹Institute of Nuclear Physics, Almaty, Kazakhstan

²Joint Institute for Nuclear Research, Dubna, Russia

e-mail: kayrat1988@bk.ru

DOI: 10.63907/ansa.v1i2.37

Received: 15 May 2025

Abstract

The two-neutron halo nucleus ^{11}Li represents one of the most striking manifestations of exotic nuclear structure far from stability. Its extremely low two-neutron separation energy, extended matter distribution, and Borromean three-body configuration ($n + n + ^9\text{Li}$) make it a benchmark system for studying weak binding, neutron correlations, and continuum effects. This review summarizes the experimental approaches that have elucidated the halo structure of ^{11}Li , including interaction cross section measurements, elastic proton scattering, transfer reactions, momentum distribution analyses, Coulomb breakup. Particular emphasis is placed on the role of the unbound subsystem ^{10}Li in shaping the structure of ^{11}Li through its virtual s -states and low-lying resonances. The experimental findings are interpreted in the context of modern three-body theoretical models, highlighting the interplay between valence neutron correlations and nuclear dynamics at the edge of stability.

Keywords: halo nucleus; ^{11}Li ; Borromean system; neutron-neutron correlation; Coulomb breakup.

1 Introduction

In recent decades, the study of weakly bound nuclei, especially those situated near the drip lines, has emerged as a key area in nuclear physics. These systems, positioned

far from the valley of beta stability, often display structural properties that challenge the conventional shell-model framework. One of the most striking features observed in such nuclei is the presence of a halo structure, where one or more loosely bound valence nucleons, typically neutrons, occupy spatially extended wavefunctions that extend well beyond the nuclear core.

One of the earliest and most compelling examples of this phenomenon is the nucleus ^{11}Li . With a two-neutron separation energy of only 369 keV [1], ^{11}Li has a neutron halo composed of two weakly bound neutrons surrounding a compact ^9Li core, see Figure 1. This unique three-body (Borromean) configuration, in which none of the binary subsystems (^{10}Li or the dineutron) are bound [2, 3], has made ^{11}Li a benchmark for halo structure studies.

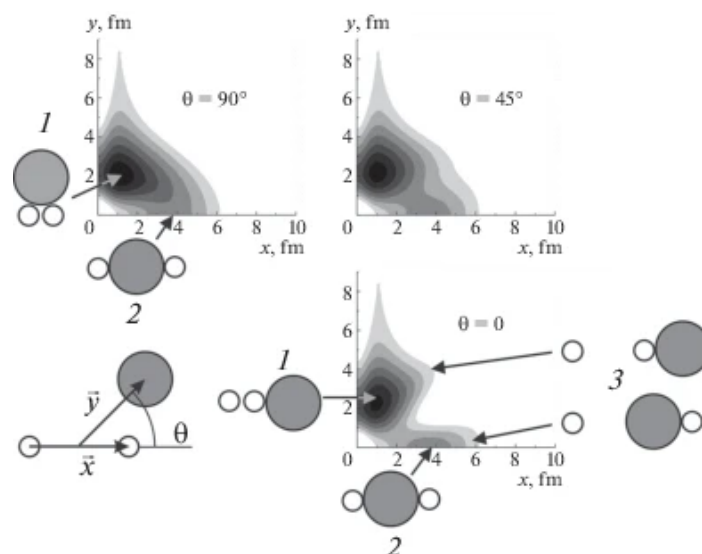


Figure 1: Probability density in Jacobi coordinates x, y with examples of neutron positions (white circles) and ^9Li positions (large gray circles); the three-body configuration of ^{11}Li ($n + n + ^9\text{Li}$) nucleus. Designations are the same as in Fig. 4. Configuration 1 with a dineutron cluster is the most probable. Linear (cigar-shaped) configuration 2 has a considerably lower probability. Configuration 3 ($n + ^{10}\text{Li}$) is even less probable, adapted from Ref. [3]

Early measurements of interaction cross sections (σ_I) in reactions involving ^{11}Li provided the first evidence for halo structures, revealing significantly increased nuclear radii compared to neighboring stable nuclei [4, 5, 6]. For example, Tanihata et al. measured σ_I for $^{11}\text{Li} + ^{12}\text{C}$ at 790 MeV/nucleon, determining an interaction radius of 3.14 fm—substantially larger than those of nearby nuclei such as ^9Li and ^{10}Be [4, 5, 7]. Subsequent elastic proton scattering experiments in inverse kinematics confirmed the extended matter distribution of ^{11}Li and were successfully interpreted using Glauber multiple scattering theory [8, 9].

The importance of studying halo nuclei lies not only in their exotic structure but also in the unique reaction dynamics they exhibit. The weak binding of halo nucleons enhances coupling to breakup and transfer channels, significantly modifying total reaction cross sections and elastic scattering angular distributions. In reactions with heavy targets, Coulomb breakup becomes especially relevant, offering a powerful tool for probing halo structure under conditions where nuclear interactions are suppressed [10, 11].

A complementary probe of the ^{11}Li halo structure at low energies was provided by measurements of total reaction cross sections for the $^{11}\text{Li} + ^{28}\text{Si}$ system in the energy range of 7–25 MeV/nucleon [12]. In this experiment, prompt gamma and neutron emissions were registered as signatures of nuclear interaction. Theoretical modeling based on the time-dependent Schrödinger equation, with explicit treatment of the weakly bound valence neutrons, successfully reproduced the observed cross sections. The agreement confirms that dynamical evolution of the halo component plays a key role in reaction mechanisms even at near-barrier energies.

Furthermore, experimental methods such as two-neutron transfer reactions [13, 14], momentum distribution studies [15, 16], and intensity interferometry techniques [18] have provided valuable and complementary information about the spatial arrangement and dynamical correlations of halo neutrons. The collected data strongly support the presence of both s -wave and p -wave components in the ground-state configuration of the ^{11}Li nucleus, along with pronounced neutron–neutron correlations that significantly influence its structural stability and binding mechanism.

The purpose of this review is to synthesize and critically evaluate the body of experimental research on light weakly bound lithium isotopes, with a particular focus on ^{11}Li . We summarize the structural properties, reaction mechanisms, and theoretical models that have emerged from studies using elastic scattering, transfer, breakup, and Coulomb excitation experiments. Particular attention is given to the role of the intermediate ^{10}Li system and its unresolved spectroscopic properties in understanding the three-body dynamics of ^{11}Li .

2 Key features of halo nuclei

A defining characteristic of halo nuclei is the significant spatial extension of their matter distribution compared to stable nuclei of similar mass. This phenomenon arises from the extremely weak binding of one or more valence neutrons, allowing their wavefunctions to extend far outside the dense nuclear core. In the case of ^{11}Li , the halo structure is formed by two valence neutrons weakly bound to a ^9Li core, resulting in a matter radius that far exceeds those of neighboring isotopes.

Initial experimental evidence for this extended structure was obtained through measurements of the interaction cross section (σ_I), which includes all processes involving nucleon removal from the projectile. In pioneering work, Tanihata and colleagues measured σ_I for $^{11}\text{Li} + ^{12}\text{C}$ at 790 MeV/nucleon and extracted a nuclear interaction radius of $R_I = 3.14$ fm [4, 1]. This value is markedly larger than those of nearby nuclei such as ^9Li (2.41 fm), ^{10}Be (2.46 fm), and ^{12}C (2.61 fm), indicating the presence of a diffuse neutron distribution [5, 7].

To probe the spatial distribution more directly, elastic scattering of ^{11}Li on proton targets at small angles was performed at GSI using beams with energies near 700 MeV/nucleon [8]. The data were analyzed using Glauber multiple scattering theory [9], which, when combined with various parameterized nuclear density profiles, reproduced the broad matter distribution consistent with a halo structure. Calculations using both Gaussian and oscillator-type densities confirmed that ^{11}Li exhibits a long density tail.

The extremely low two-neutron separation energy $S_{2n} = 369.15(65)$ keV [1] further supports the halo interpretation. The small binding energy implies that the two halo neutrons are only marginally bound and can be easily removed, enhancing

their spatial delocalization. This property plays a critical role in shaping both the size and dynamical behavior of the system.

Structurally, ^{11}Li is an archetype of a Borromean nucleus—a three-body bound state ($n + n + ^9\text{Li}$) in which none of the two-body subsystems ($n + n$, $^9\text{Li} + n$) are themselves bound [2, 3]. This means that the removal of any one component leads to an unbound system. The Borromean nature of ^{11}Li was confirmed by theoretical studies using Jacobi coordinate systems to analyze the three-body probability distribution [3, 19]. These studies show that the most probable configuration involves a dineutron-like cluster, although linear (cigar-like) and core-neutron cluster configurations are also present with lower probability.

The three-body character of ^{11}Li has important implications for theoretical modeling and experimental observables. It requires explicit treatment of core-halo and neutron-neutron correlations, which are essential to reproduce observables such as angular distributions in transfer reactions and momentum profiles of breakup fragments. Furthermore, the structure of ^{11}Li has a direct bearing on the spectroscopy of ^{10}Li , since its unbound nature prevents it from being a well-defined subsystem, yet it governs the n -core interaction in the halo nucleus.

The extended matter distribution, extremely low binding energy, and Borromean nature of ^{11}Li make it a canonical system for studying halo phenomena. Its unique three-body structure continues to provide insights into the interplay between nuclear forces, quantum few-body dynamics, and continuum coupling near the drip lines.

The key physical parameters of the two-neutron halo nucleus ^{11}Li and its neighboring isotopes are summarized in Table 1. These include two-neutron separation energy, interaction radius, matter radius, momentum distribution width of breakup fragments, and experimental evidence for neutron-neutron correlations. The comparison with nearby stable nuclei such as ^9Li , ^{10}Be , and ^{12}C highlights the unique extended structure of ^{11}Li and confirms its status as a benchmark halo nucleus.

Table 1: Key physical parameters of ^{11}Li and neighboring isotopes: two-neutron separation energy S_{2n} , interaction radius R_I , matter radius R_m , FWHM of longitudinal momentum distribution (LMD) of ^9Li fragments, and neutron-neutron correlation distance from HBT interferometry.

Isotope	S_{2n} (keV)	R_I (fm)	R_m (fm)	LMD FWHM (MeV/c)	nn RMS dist. (fm)	Reference(s)
^{11}Li	369.15	3.14	~ 3.5	47	6.6 ± 1.5	[1, 4, 5, 8, 15–17]
^9Li	—	2.41	—	>150	—	[5, 7]
^{10}Be	—	2.46	—	—	—	[5]
^{12}C	—	2.61	—	—	—	[7]

3 Experimental approaches to halo nuclei

3.1 Interaction cross sections

One of the most powerful and historically important tools in identifying halo structures in exotic nuclei has been the measurement of total interaction cross sections (σ_I). These cross sections, which encompass all processes that remove one or more nucleons from the projectile nucleus, provide a direct and model-independent measure of the spatial extension of the nuclear matter distribution.

In the mid-1980s, pioneering measurements at RIKEN revealed that neutron-rich light nuclei such as ^{11}Li possess unexpectedly large interaction cross sections when scattered off a ^{12}C target at high energies [4, 5]. The beam energy of 790 MeV/nucleon was sufficiently high to allow for the use of the eikonal approximation, and the observed σ_I for ^{11}Li was measured to be approximately 1060 mb [1].

The significance of this measurement lies in its clear deviation from systematics based on stable nuclei. For comparison, the interaction radii of neighboring nuclei were significantly smaller: $R_I(^9\text{Li}) = 2.41$ fm, $R_I(^{10}\text{Be}) = 2.46$ fm, and $R_I(^{12}\text{C}) = 2.61$ fm [5, 7]. In contrast, ^{11}Li exhibited an interaction radius of $R_I = 3.14$ fm, implying an anomalously large spatial extent of the matter distribution. This result was interpreted as the first compelling evidence of a neutron halo: a diffuse distribution of valence neutrons surrounding a tightly bound core.

Theoretical modeling of σ_I using the Glauber multiple scattering formalism allowed these experimental observations to be quantitatively linked to the radial density profiles of the projectile nucleus [9]. For ^{11}Li , the best agreement with data was achieved by assuming a two-component density distribution with a compact ^9Li core and a spatially extended neutron halo. The effect of the halo manifests in the long tails of the density profile, which significantly enhances the interaction cross section.

The value of σ_I as an observable is further enhanced by its robustness and relative ease of measurement, even for short-lived nuclei with half-lives of a few milliseconds. This has allowed systematic studies across isotopic chains, confirming that the sharp increase in σ_I observed for ^{11}Li is unique among lithium isotopes. Additionally, the low two-neutron separation energy $S_{2n} = 369$ keV [1] supports the interpretation of weakly bound halo neutrons that dominate the outer density.

The nuclear interaction radius R_I is a key parameter extracted from total interaction cross section (σ_I) measurements, reflecting the effective size of the nucleus as “seen” in high-energy reactions. For halo nuclei, this value significantly exceeds expectations based on conventional nuclear systematics, due to the diffuse distribution of weakly bound neutrons.

In the case of ^{11}Li , the first precise determination of R_I was performed by Tanihata et al. through measurements of σ_I at 790 MeV/nucleon on a ^{12}C target [4, 5]. The interaction cross section for ^{11}Li was measured to be 1060 mb [1], which was significantly larger than for neighboring isotopes. Using a Glauber model framework with optical limit approximation and effective nucleon-nucleon interactions, the measured σ_I was converted into an interaction radius of $R_I = 3.14$ fm.

This value is exceptional: it surpasses those of nearby isotopes such as ^9Li (2.41 fm) and ^{10}Be (2.46 fm) [5, 7], and even that of stable ^{12}C (2.61 fm). The large R_I of ^{11}Li was one of the earliest indicators of its extended matter distribution and the presence of a halo composed of two weakly bound neutrons.

The extraction of R_I is model-dependent to some extent, particularly sensitive to the assumed density profiles. Nonetheless, the magnitude of the enhancement for ^{11}Li was too large to be accounted for by any reasonable modification of the core structure alone. Subsequent calculations incorporating a two-component density (core plus halo) provided a much better fit to the observed σ_I , confirming the physical reality of the halo structure [9].

Further supporting evidence comes from independent approaches, including elastic scattering [8] and momentum distribution measurements [15], all converging on a picture in which ^{11}Li exhibits a neutron distribution extending well beyond the range of conventional nuclear forces.

Thus, the determination of the nuclear interaction radius from σ_I measurements not only quantitatively demonstrated the anomalous size of ^{11}Li , but also played a crucial role in identifying it as a benchmark halo nucleus.

3.2 Elastic scattering experiments

Elastic scattering of exotic nuclei in inverse kinematics has proven to be an essential tool in the investigation of halo structures, particularly for short-lived radioactive beams. Unlike total interaction cross sections, elastic scattering provides more differential information, allowing researchers to extract radial matter density distributions with better spatial resolution and model discrimination. In the context of ^{11}Li , elastic proton scattering has played a critical role in confirming the extended neutron distribution inferred from interaction cross section measurements.

Pioneering experiments were carried out at GSI, where ^{11}Li beams at 62 MeV/nucleon and 68 MeV/nucleon were scattered off hydrogen targets in inverse kinematics [8]. These measurements focused on the angular distributions of the scattered protons in the center-of-mass system, particularly in the region of small momentum transfer ($q \approx 0.1 - 0.5 \text{ fm}^{-1}$), where sensitivity to the halo region is greatest.

To interpret the experimental results, the Glauber multiple scattering theory was employed [9]. This formalism allows for the extraction of the matter density distribution from the elastic scattering cross section by folding effective nucleon-nucleon interactions with parameterized nucleon density profiles. In the case of ^{11}Li , density profiles were modeled using various assumptions, such as Gaussian or harmonic oscillator distributions for the core, combined with extended distributions for the valence neutrons.

The analysis confirmed a matter radius for ^{11}Li of approximately 3.53 fm, consistent with the earlier σ_I -based estimates [1]. Importantly, the halo component was found to dominate the scattering at low momentum transfer, highlighting the presence of a long tail in the matter density. The corresponding density distributions, plotted as a function of radial distance, clearly showed a two-component structure: a compact ^9Li -like core and a significantly more extended halo [8].

Moreover, the model fits revealed that the root-mean-square (rms) radius of the halo neutrons alone exceeds 5.0 fm, an extraordinary result for such a light nucleus. These findings were further supported by comparisons to reference nuclei without halo structures, such as ^9Li and ^{12}C , which exhibited much sharper fall-offs in the elastic scattering cross sections [7].

Elastic scattering thus provided critical validation of the halo picture in ^{11}Li

and offered a more detailed understanding of the spatial structure of both the core and the valence neutrons. When used in conjunction with other probes—such as interaction cross sections, transfer reactions, and breakup measurements—elastic scattering completes a coherent and quantitatively consistent view of the halo nucleus ^{11}Li .

3.3 Nucleon transfer reactions

Nucleon transfer reactions are among the most informative probes of nuclear structure, offering detailed spectroscopic insight into single-particle configurations and nucleon correlations. For halo nuclei like ^{11}Li , such reactions are particularly valuable because they allow investigation of the underlying dynamics and structure of the valence neutrons and the nature of the coupling to the core.

One of the most informative studies of transfer reactions involving ^{11}Li is the two-neutron process $^1\text{H}(^{11}\text{Li}, ^9\text{Li})^3\text{H}$, conducted at TRIUMF with a radioactive ^{11}Li beam at 3MeV/nucleon [13, 14]. The experiment involved measuring angular distributions of the outgoing particles in order to probe the underlying structure of ^{11}Li and investigate the spatial configuration and correlations of the transferred neutrons.

Differential cross sections for transitions to the ground state ($\frac{3}{2}^-$) and first excited state ($\frac{1}{2}^-$) of ^9Li were compared with distorted-wave Born approximation (DWBA) calculations. The observed angular patterns were inconsistent with models based on uncorrelated, stepwise transfer mechanisms. Instead, the data indicated a dominant contribution from a correlated neutron pair—commonly referred to as a dineutron-like cluster [14].

These findings offer compelling evidence for strong neutron–neutron correlations within the halo of ^{11}Li , as well as a prominent s -wave component in its ground-state wave function. The angular distributions support a structural picture of ^{11}Li comprising a mixture of $(s_{1/2})^2$ and $(p_{1/2})^2$ neutron configurations coupled to the ^9Li core [14].

The ability to populate different final states in ^9Li further highlighted the sensitivity of the transfer reaction to the initial halo configuration and provided constraints on theoretical models describing ^{11}Li as a three-body system. This included the influence of continuum effects and final-state interactions in the ^{10}Li intermediate system, which plays a key role in the halo structure.

Importantly, the results from transfer reactions complemented findings from interaction cross section and elastic scattering studies. While those approaches revealed the extended spatial structure of the halo, the transfer reaction offered unique insight into the quantum mechanical structure and correlations of the two neutrons.

In conclusion, nucleon transfer reactions such as $^1\text{H}(^{11}\text{Li}, ^9\text{Li})^3\text{H}$ are indispensable tools for understanding the pairing and orbital structure of halo neutrons in ^{11}Li . The experimental results strongly support the picture of a spatially extended, correlated two-neutron halo and have become a benchmark for testing modern three-body and shell-model–based descriptions of exotic light nuclei.

3.4 Momentum distributions of fragments

A key signature of two-neutron halo nuclei is the extremely small two-neutron separation energy, which leads to unique decay dynamics in nucleon removal reactions. For ^{11}Li , the two-neutron separation energy is only 369.25 keV, and the mass- $A-1$ nucleus (^{10}Li) is unbound [1]. As a result, one-neutron removal from ^{11}Li leads to rapid decay of the intermediate system into the core (^9Li) and a neutron. This pattern is characteristic of other Borromean halo nuclei, including $^{6,8}\text{He}$, ^{14}Be , and $^{17,19}\text{B}$, where fragment detection in reactions usually involves only the strongly bound core.

One of the most direct experimental techniques to probe the spatial structure of halo nuclei is the measurement of fragment momentum distributions following neutron knockout [15]. According to the Heisenberg uncertainty principle, the extended spatial distribution of the halo should result in a narrow momentum spread of the core fragment. For ^{11}Li , transverse and longitudinal momentum distributions of ^9Li fragments have been measured at 280 MeV/nucleon on ^{12}C , ^{27}Al , and ^{208}Pb targets [16], see Figure 2. In all cases, the observed momentum widths were approximately 47 MeV/ c , significantly narrower than the ~ 100 MeV/ c expected for well-bound nuclei [17], indicating a spatially extended halo structure.

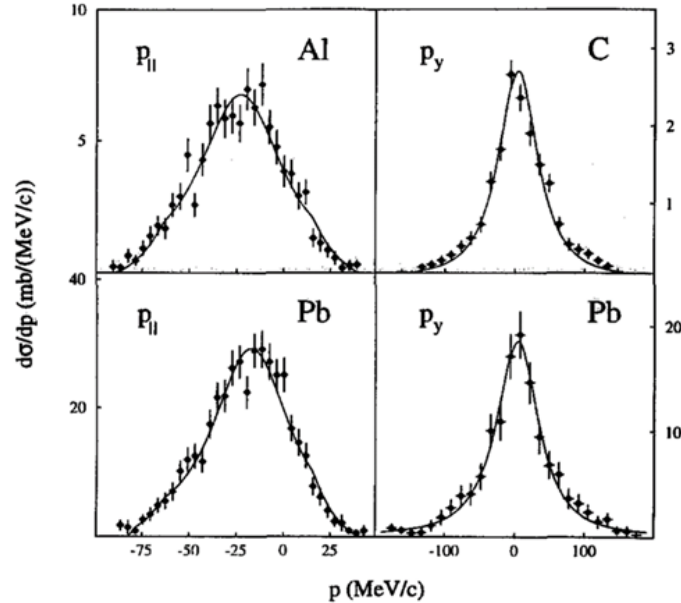


Figure 2: Longitudinal (p_{\parallel}) and transverse (p_y) momentum distributions of ^9Li fragments resulting from the breakup of ^{11}Li on ^{12}C , ^{27}Al , and ^{208}Pb targets at 280 MeV/nucleon, adapted from Ref. [16].

Furthermore, the reactions involving halo neutron removal were found to occur at relatively large impact parameters implying peripheral interactions [15, 16]. This is in contrast to strongly interacting systems, where smaller impact parameters lead to fusion or deep inelastic reactions. Thus, momentum distribution measurements not only confirm the extended spatial nature of ^{11}Li , but also provide insight into the geometry of the reaction mechanism.

3.5 Coulomb excitation and breakup

Coulomb excitation and breakup reactions are critical tools for probing the structure of halo nuclei like ^{11}Li , especially due to their sensitivity to the electric dipole ($E1$) response, see Figure 3. When ^{11}Li interacts with a high- Z target such as Pb, the strong electromagnetic field can induce breakup of the loosely bound system, providing insight into the dynamics of valence neutrons.

Experiments performed at intermediate and high energies using ^{11}Li beams have revealed enhanced $E1$ strength at low excitation energies, consistent with expectations for a soft dipole mode arising from the oscillation of halo neutrons against the ^9Li core [10, 11]. For example, in the $^{11}\text{Li} + ^{208}\text{Pb}$ reaction at 64 MeV/nucleon, the Coulomb breakup cross section was measured as a function of the relative energy of decay fragments, showing a pronounced peak at low E_{rel} values [10]. This structure reflects strong dipole transitions into the continuum, a hallmark of halo systems.

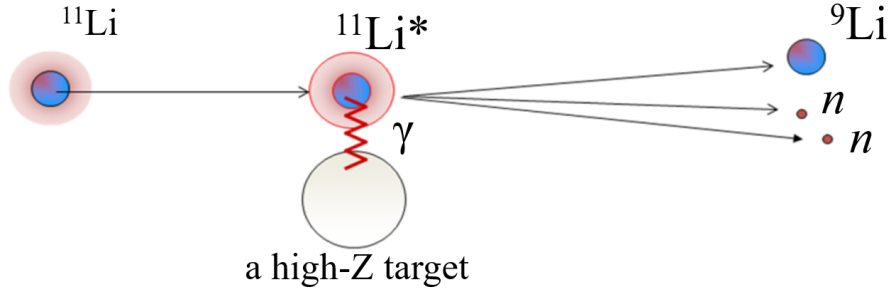


Figure 3: Breakup of the ^{11}Li nucleus induced by Coulomb excitation on a high- Z target, leading to the emission of two halo neutrons and the ^9Li core.

To isolate the Coulomb contribution, comparative measurements were made using light targets like carbon, where nuclear breakup dominates, and heavy targets like lead, where electromagnetic interaction is enhanced [11]. The difference in observed cross sections between these systems confirms the predominance of Coulomb excitation in the $^{11}\text{Li} + \text{Pb}$ channel at forward angles and low excitation energies.

Moreover, fully kinematic measurements detecting both ^9Li and neutrons in coincidence have been performed to investigate correlations in the final state [20, 21, 22]. These experiments provided valuable insight into the three-body continuum of ^{11}Li and allowed a direct probe of neutron–neutron spatial correlations. Analysis of the angular and energy spectra of the outgoing neutrons revealed clear deviations from models assuming uncorrelated emission. The results point toward a strongly correlated emission pattern of the two halo neutrons, suggesting that they are released in close proximity — consistent with a compact, dineutron-like structure [21, 22].

The analysis of the relative energy spectra of $^9\text{Li} + n + n$ systems further supported the Borromean nature of ^{11}Li and revealed a strong final-state interaction peak in the low-energy region [21]. These observables, such as the narrow relative energy distributions and back-to-back emission of neutrons, are direct experimental signatures of halo decay dynamics.

3.6 Neutron-neutron correlations in ^{11}Li from HBT interferometry

The spatial correlation between the two valence neutrons in halo nuclei such as ^{11}Li has been the subject of growing interest. One of the most direct and model-independent techniques to probe such correlations is Hanbury Brown–Twiss (HBT) intensity interferometry [23, 24]. Originally developed in astrophysics to determine the angular diameter of distant radio sources, the method has been extensively adapted for nuclear physics to extract information about the spatial and temporal characteristics of the particle-emitting source in high-energy collisions.

In nuclear applications, the HBT method constructs a two-particle correlation function from pairs of emitted neutrons, protons, pions, or light ions. When applied to the breakup of ^{11}Li , HBT interferometry allows direct investigation of the spatial separation between the two halo neutrons at the time of emission, offering insight into the intrinsic structure of the nucleus.

The pioneering application of this technique to ^{11}Li breakup was reported in [18], where neutron-neutron correlation functions were measured following reactions on light targets. From the shape of the correlation function, the root-mean-square (rms) distance between the two neutrons in the halo was extracted to be approximately 6.6 ± 1.5 fm [18] (Figure 4). This experimental value was found to be in good agreement with three-body model calculations [25], which predict a neutron–neutron rms separation of about 6.7 – 8.3 fm.

Given the previously established interaction radius of ^{11}Li , $R_I = 3.14$ fm [1], and the characteristic matter radius of the core–halo system, the HBT result implies a mostly linear (cigar-like) configuration of the two halo neutrons and the ^9Li core. Such a geometry places the neutrons predominantly on opposite sides of the core, supporting a spatially extended, quasi-linear three-body configuration. However, theoretical models suggest that this specific arrangement, although consistent with the data, may not be the most probable configuration in the full quantum three-body wavefunction [3].

4 The role of ^{10}Li in Understanding ^{11}Li

The unbound nucleus ^{10}Li plays a central role in the structure and theoretical interpretation of ^{11}Li , as it serves as the intermediate two-body subsystem in the Borromean three-body configuration: $^{11}\text{Li} \equiv ^9\text{Li} + n + n$. Understanding the low-lying states and neutron-core interaction in ^{10}Li is therefore essential for accurate three-body modeling of the ^{11}Li halo.

Unlike ^{11}Li , ^{10}Li is unbound and does not exist as a stable or resonant nucleus. Its structure must instead be inferred indirectly from reactions such as neutron transfer, fragmentation, and breakup of ^{11}Li . Experimental studies have revealed low-energy virtual s -wave states and possible p -wave resonances near threshold [2, 3].

Measurements of $^9\text{Li}(d,p)^{10}\text{Li}$ and other transfer-type reactions provide evidence for a strong s -wave component in the ^{10}Li spectrum. The virtual nature of this state, characterized by a negative scattering length, is essential in reproducing the large spatial extension of the halo neutrons in ^{11}Li [2].

The ambiguity in the ^{10}Li spectrum directly affects theoretical descriptions of ^{11}Li . Since ^{11}Li is bound while ^{10}Li is not, the neutron-neutron and neutron-core

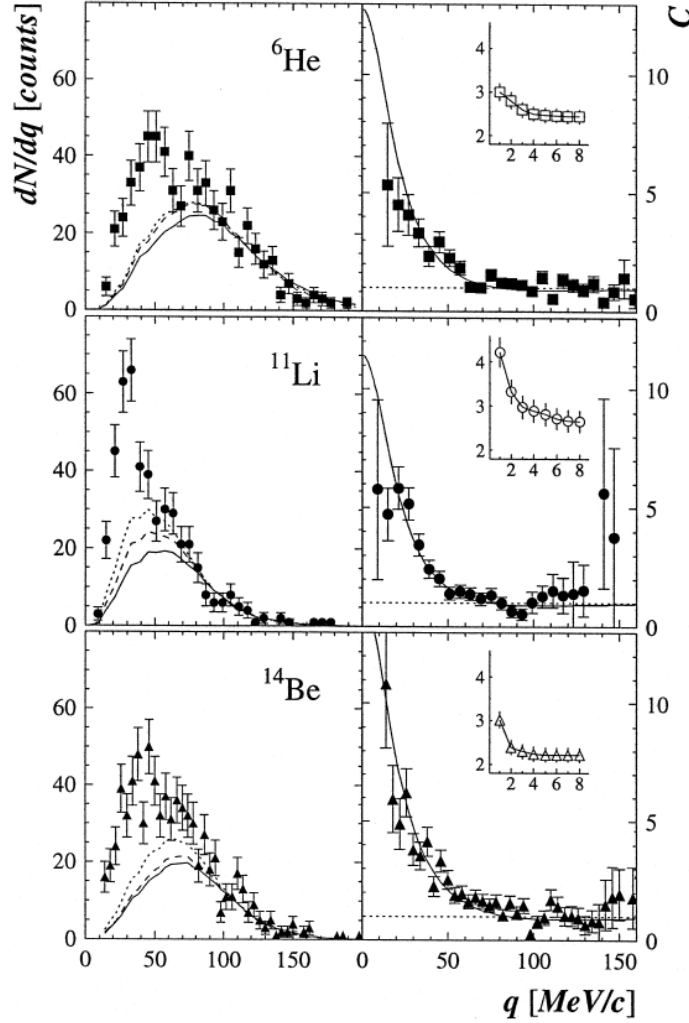


Figure 4: Neutron-neutron correlation function $C(q)$ for the dissociation of ^{11}Li , extracted using the HBT analysis. Adapted from [18]

interactions must be fine-tuned to reproduce the correct separation energy and matter radius of ^{11}Li . Three-body models using Jacobi coordinates demonstrate that different assumptions about the virtual s -state and p -resonance in ^{10}Li lead to significantly different predictions for the halo configuration and the nature of dineutron correlations [19].

Moreover, the reaction observables such as momentum distributions, Coulomb breakup spectra, and transfer cross sections are all sensitive to the properties of ^{10}Li . For example, the soft dipole mode observed in Coulomb excitation experiments is shaped by the accessibility of low-lying continuum states in ^{10}Li , which guide the breakup of ^{11}Li into $^9\text{Li} + n + n$ [11, 21].

In summary, ^{10}Li serves as a crucial anchor point for understanding the structure of ^{11}Li . Although it is unbound, its virtual and resonant states govern the effective neutron-core interaction that binds the halo system. Accurate modeling of ^{10}Li is therefore indispensable for any realistic theoretical treatment of ^{11}Li and provides an essential link between experiment and few-body theory.

5 Recent reaction-based probes of ^{11}Li structure

Reactions in inverse kinematics offer direct insight into the halo structure of ^{11}Li beyond global observables like interaction cross sections. Recent experiments and models have focused on spin-isospin excitations, neutron correlations, and continuum structure.

At RIKEN's RIBF, the $^{11}\text{Li}(p, n)^{11}\text{Be}$ reaction was studied using the SAMURAI spectrometer and PANDORA neutron detector. Multiple decay channels, including $1n$, $2n$, d , t , 2α , and $^6\text{He} + \alpha$, were observed, reflecting the complex continuum of ^{11}Be and its link to the halo structure of ^{11}Li [26].

Opening angle distributions in (p, pn) knockout reactions have emerged as sensitive probes of dineutron correlations. Theoretical studies show this observable is robust at low intrinsic momenta and mostly model-independent, but subject to distortion effects at higher momenta [27].

Elastic scattering of ^{11}Li on ^{12}C and ^{28}Si at intermediate energies has been successfully modeled using double folding optical potentials. Calculations using the CDM3Y6 interaction reproduce angular distributions and cross sections, confirming the large spatial extent of the nucleus [28].

A new experimental proposal aims to populate excited states of ^{11}Li via the $^9\text{Li}(t, p)$ reaction at ISOLDE. Using a novel Si-telescope setup, this approach offers improved resolution and may resolve long-standing questions about the halo nucleus's excitation spectrum [29].

Theoretical investigations of two-neutron halo systems, such as ^{11}Li and ^{22}C , have highlighted the sensitivity of ground-state configuration mixing to the neutron-core interaction potential. Singh and Horiuchi employed a three-body model (core+ $n+n$) incorporating explicit coupling to the unbound continuum of the core+ n subsystem [30]. Using a density-dependent contact-delta interaction to model the neutron-neutron force, they adjusted its strength to match the experimental binding energies. Their results show that the degree of $s-p$ mixing in the ground state of ^{11}Li depends sensitively on the strength and shape of the core-neutron potential, with implications for both dineutron correlations and halo spatial structure.

Theoretical models based on three-body frameworks have played a central role in elucidating the structure of Borromean halo nuclei, such as ^{11}Li . In particular, the work of Bhasin and Mazumdar offers an extensive overview of developments over the past two decades involving separable interactions within this formalism [31]. Their review highlighted the effectiveness of such models in reproducing essential observables for ^{11}Li , including its binding energy, spatial extension (matter radius), momentum profiles, neutron-neutron correlation features, and decay behavior. Additionally, the discussion extended to predictions of Efimov-like states in heavier halo systems such as ^{14}Be , ^{22}C , and ^{19}B , with particular emphasis on the identification of a near-threshold virtual state in ^{13}Be , which holds significance for understanding the structure of ^{14}Be . These results underscore the relevance of few-body theoretical approaches in describing the universal properties of loosely bound nuclear systems near the drip line.

Elastic electron scattering has emerged as a promising method for probing the charge distributions of halo nuclei with high spatial resolution. Ridha and Majeed conducted theoretical calculations of elastic electron scattering form factors for several halo systems, including ^{11}Li , within a core+halo framework [32]. The model

combined harmonic oscillator wave functions for the core and Woods–Saxon potentials for the valence halo nucleons. For ^{11}Li , the approach successfully reproduced the long density tail and root-mean-square radius consistent with experimental data. Their calculated monopole (C0) form factors offer valuable predictions for future electron–radioactive ion beam scattering experiments, potentially enabling direct imaging of the extended neutron distributions in halo systems.

6 Conclusion

The lithium isotope ^{11}Li has become a cornerstone in the study of exotic nuclear structure, particularly due to its status as a canonical two-neutron halo nucleus and a prime example of a Borromean system. Its extremely low two-neutron separation energy, extended matter distribution, and strong neutron-neutron correlations challenge traditional shell-model paradigms and offer a unique testing ground for few-body quantum systems at the limits of nuclear binding.

A diverse array of experimental approaches have all converged on a coherent picture of ^{11}Li as a spatially extended, weakly bound three-body system with a compact ^9Li core and two correlated halo neutrons. These experiments have revealed distinctive observables: large interaction radii, narrow momentum distributions, enhanced low-energy $E1$ strength, and strong $n-n$ correlations.

The unbound ^{10}Li subsystem plays a crucial role in understanding the structure of ^{11}Li . Its virtual s -state and possible low-lying p -resonances govern the neutron-core interaction, which must be accurately modeled to reproduce the binding and configuration of the halo. This interdependence highlights the importance of unified three-body theoretical frameworks and motivates continued efforts in improving our understanding of interactions near the neutron drip line.

In summary, ^{11}Li continues to serve as a benchmark system for exploring the interplay between nuclear forces, quantum correlations, and continuum effects in weakly bound nuclei. Ongoing and future experiments with improved radioactive beam intensities, higher-resolution detectors, and more refined reaction models promise to further unravel the complexity of halo systems and extend our understanding to even more exotic regions of the nuclear chart.

References

- [1] M. Smith, M. Brodeur, T. Brunner et al., *Phys. Rev. Lett.* **101**, 202501 (2008).
- [2] R.M. Id Betan, *Nucl. Phys. A* **959**, 147 (2017).
- [3] V.V. Samarin, M.A. Naumenko, *Bull. Russ. Acad. Sci.: Phys.* **83**(4), 411 (2019).
- [4] I. Tanihata, H. Hamagaki, O. Hashimoto et al., *Phys. Lett. B* **160**, 380 (1985).
- [5] I. Tanihata, H. Hamagaki, O. Hashimoto et al., *Phys. Rev. Lett.* **55**, 2676 (1985).
- [6] I. Tanihata, T. Kobayashi, O. Yamakawa et al., *Phys. Lett. B* **206**, 592 (1988).
- [7] J. Jaros, A. Wagner, L. Anderson et al., *Phys. Rev. C* **18**, 2273 (1978).

- [8] P. Egelhof, G.D. Alkhazov, M.N. Andronenko et al., *Eur. Phys. J. A* **15**, 27 (2002).
- [9] S.L. Alkhazov, G.D. Belostotsky, A.A. Vorobyov, *Phys. Rep.* **42**, 89 (1978).
- [10] I. Tanihata, C. Savajols, R. Kanungo, *Prog. Part. Nucl. Phys.* **68**, 215 (2013).
- [11] T. Kobayashi, S. Shimoura, I. Tanihata et al., *Phys. Lett. B* **232**, 51 (1989).
- [12] Yu.E. Penionzhkevich, Yu.G. Sobolev, V.V. Samarin, M.A. Naumenko, N.A. Lashmanov, V.A. Maslov, I. Siváček, S.S. Stukalov, *Phys. Rev. C* **99**, 014609 (2019).
- [13] I. Tanihata, M. Alcorta, D. Bandyopadhyay et al., *Phys. Rev. Lett.* **100**, 192502 (2008).
- [14] G. Potel, F. Barranco, E. Vigezzi, R.A. Broglia, *Phys. Rev. Lett.* **105**, 172502 (2010).
- [15] P.G. Hansen, *Phys. Rev. Lett.* **77**, 1016 (1996).
- [16] F. Humbert, T. Nilsson, W. Schwab et al., *Phys. Lett. B* **347**, 198 (1995).
- [17] A.S. Goldhaber, *Phys. Lett. B* **53**, 306 (1974).
- [18] F. Marqués, M. Labiche, N. Orr et al., *Phys. Lett. B* **476**, 219 (2000).
- [19] D.I. Blokhintsev, *Principles of Quantum Mechanics*, Boston: Allyn and Bacon, 1964, 620 p.
- [20] D. Aleksandrov, T. Aumann, L. Axelsson et al., *Nucl. Phys. A* **669**, 51 (2000).
- [21] R. Palit, P. Adrich, T. Aumann et al., *Phys. Rev. C* **68**, 034318 (2003).
- [22] M. Labiche, N.A. Orr, F.M. Marqués et al., *Phys. Rev. Lett.* **86**, 600 (2001).
- [23] D.H. Boal, C.-K. Gelbke, B.K. Jennings, *Rev. Mod. Phys.* **62**, 553 (1990).
- [24] D.H. Hoal, H. DeGuise, *Phys. Rev. Lett.* **57**, 2901 (1986).
- [25] M.V. Zhukov, B.V. Danilin, D.V. Fedorov et al., *Phys. Rep.* **231**, 151 (1993).
- [26] S. Miyazaki, T. Nakamura, Y. Kondo et al., *J. Phys. Conf. Ser.* **1643**, 012107 (2020).
- [27] M. Rodríguez-Gallardo, J. Casal, A.M. Moro, *Phys. Rev. C* **104**, 024618 (2021).
- [28] M.A. Yousif, A.M. Hassan, *Chin. Phys. C* **44**, 124105 (2020).
- [29] J. Carbajo et al., *EPJ Web Conf.* **290**, 02010 (2023).
- [30] J. Singh, W. Horiuchi, *J. Phys.: Conf. Ser.* **1643**, 012158 (2020).
- [31] V.S. Bhasin, I. Mazumdar, *Three-Body Approach to Structural Properties of Halo Nuclei and the Efimov Effect*, in: *Few Body Dynamics, Efimov Effect and Halo Nuclei*, SpringerBriefs in Physics (2020), pp. 69–119.
- [32] A.R. Ridha, W.Z. Majeed, *Iraqi J. Sci.* **63**(3), 1097 (2022).